



# Protective effect of baicalin against arsenic trioxide-induced acute hepatic injury in mice through JAK2/STAT3 signaling pathway

International Journal of  
Immunopathology and Pharmacology  
Volume 36: 1–14  
© The Author(s) 2022  
Article reuse guidelines:  
[sagepub.com/journals-permissions](https://sagepub.com/journals-permissions)  
DOI: 10.1177/20587384211073397  
[journals.sagepub.com/home/iji](https://journals.sagepub.com/home/iji)  
SAGE

Qianqian He<sup>1</sup>, Xiaoqi Sun<sup>1</sup>, Muqing Zhang<sup>2,3</sup>, Li Chu<sup>1,4</sup> , Yang Zhao<sup>5</sup>, Yongchao Wu<sup>5</sup>, Jianping Zhang<sup>4,6</sup>, Xue Han<sup>1,2</sup>, Shengjiang Guan<sup>2,6</sup>  and Chao Ding<sup>7</sup>

## Abstract

Baicalin (BA) is a kind of flavonoid that is isolated from *Scutellaria baicalensis* Georgi, which has been verified to have hepatoprotective effects in some diseases. However, the role of BA in acute hepatic injury induced by arsenic trioxide (ATO) remains unclear. The aim of this study was to investigate the protective action of BA on acute hepatic injury induced by ATO and to probe its possible mechanism. Mice were pretreated with BA (50, 100 mg/kg) by gavage. After 7 h, ATO (7.5 mg/kg) was injected intraperitoneally to induce liver injury. After 7 days of treatment, serum and hepatic specimens were collected and assayed to evaluate the hepatoprotective effect of BA. Pathological sections and the liver function index indicated that ATO caused significant liver injury. The fluorescence of reactive oxygen species and oxidative stress indicators showed that ATO also increased oxidative stress. The inflammatory markers in ATO-induced mice also increased significantly. Staining of the terminal deoxynucleotidyl transferase dUTP nick end labeling and apoptotic factor assay showed that apoptosis increased. However, with BA pretreatment, these changes were significantly weakened. In addition, BA treatment promoted the expression of proteins related to the JAK2/STAT3 signaling pathway. The results suggest that BA can ameliorate acute ATO-induced hepatic injury in mice, which is related to the inhibition of oxidative stress, thereby reducing inflammation and apoptosis. The mechanism of this protection is potentially related to the JAK2/STAT3 signaling pathway.

## Keywords

baicalin, arsenic trioxide, acute hepatic injury, oxidative stress, apoptosis, JAK2/STAT3

Date received: 29 September 2021; accepted: 23 December 2021

<sup>1</sup>School of Pharmacy, Hebei University of Chinese Medicine, Shijiazhuang, China

<sup>2</sup>Affiliated Hospital, Hebei University of Chinese Medicine, Shijiazhuang, China

<sup>3</sup>College of Integrative Medicine, Hebei University of Chinese Medicine, Shijiazhuang, China

<sup>4</sup>Hebei Key Laboratory of Integrative Medicine on Liver-Kidney Patterns, Shijiazhuang, China

<sup>5</sup>The Fourth Hospital of Hebei Medical University, Shijiazhuang, China

<sup>6</sup>School of Basic Medicine, Hebei University of Chinese Medicine, Shijiazhuang, China

<sup>7</sup>Department of Cardiology, Bethune International Peace Hospital of PLA, Shijiazhuang, China

## Corresponding authors:

Shengjiang Guan, Affiliated Hospital, Hebei University of Chinese Medicine, No. 3, Xingyuan Road, Luquan Economic Development Zone, Luquan District, Shijiazhuang, Hebei 050011, China.

Email: [guanshengjiang123@126.com](mailto:guanshengjiang123@126.com)

Chao Ding, Department of Cardiology, Bethune International Peace Hospital of PLA, Shijiazhuang, Hebei 050011, China. Email [dingch2001@163.com](mailto:dingch2001@163.com)



Creative Commons Non Commercial CC BY-NC: This article is distributed under the terms of the Creative Commons Attribution-NonCommercial 4.0 License (<https://creativecommons.org/licenses/by-nc/4.0/>) which permits non-commercial use, reproduction and distribution of the work without further permission provided the original work is attributed as specified on the SAGE and Open Access pages (<https://us.sagepub.com/en-us/nam/open-access-at-sage>).

## Introduction

Arsenic (As) is a hazardous metalloid that is found in soil, air, and water, where it mainly occurs in the form of oxides or sulfides.<sup>1</sup> Studies have shown that As causes pathological changes by enhancing oxidative stress.<sup>2</sup> Among the many As compounds, arsenic trioxide (ATO) has attracted the most attention as a monotherapy or in combination with all-trans-retinoic acid and anthracyclines for acute promyelocytic leukemia (APL).<sup>3</sup> However, the use of ATO is often associated with serious side effects. Studies show that exposure to ATO can cause a variety of toxic effects, such as hepatotoxicity, neurotoxicity, nephrotoxicity, and cardiotoxicity, which limit its clinical use.<sup>4</sup>

The liver is an important organ that participates in the metabolism and excretion of various biochemical substances in the human body. It plays roles in deoxygenation, storage of liver sugar, and secretion of synthesized proteins. It is also the body's largest detoxification organ, and many chemotherapy drugs are metabolized by liver enzymes.<sup>5</sup> Because of its anatomical location and metabolic properties, it is vulnerable to a variety of toxic substances. Therefore, the liver is one of the main target organs of ATO.<sup>6</sup> After ATO enters the liver, reactive oxygen species (ROS) is produced, which causes oxidative stress and leads to liver damage.<sup>7</sup> Two clinical trials on APL also report that 25–63% of patients who received ATO and all-trans-retinoic acid therapy developed grade 3–4 hepatotoxicity.<sup>8,9</sup>

In recent years, people have paid more attention to natural medicine, and one of our goals is to find out whether there are good liver-protection drugs and ingredients from traditional Chinese medicine. *Scutellaria baicalensis* Georgi is one of the commonly used traditional Chinese medicines, and its dried root is used for clearing heat and dampness, purging fire and detoxification, hemostasis, and fetal protection.<sup>10</sup> Baicalin (BA) (5,6,7-trihydroxyflavone-7-beta-D-glucuronic acid) (Figure 1) is one of the most effective and abundant polyphenolics extracted from the root.<sup>11,12</sup> In a number of in vitro and in vivo studies, BA has been proven to have a variety of pharmacological effects, such as anti-oxidation, anti-inflammation, anti-microbial, and anti-cancer effects.<sup>13</sup> Many experiments have proven that BA can play an excellent protective role in different injuries caused by alcohol, iron overload, ischemia-reperfusion, cholestasis, and other conditions.<sup>14–17</sup> However, it is unclear whether BA also has a protective effect against ATO-induced acute liver injury.

It has been suggested that enhancing anti-apoptosis and proliferation of liver cells is the key to protecting the liver through STAT3.<sup>18</sup> This has provided an idea for us to explore the mechanism of liver protection by BA. STATs are “signal transducers and activators of transcription” and play a crucial role in signal transduction and transcriptional activation. STAT3 is a member of the STAT family of

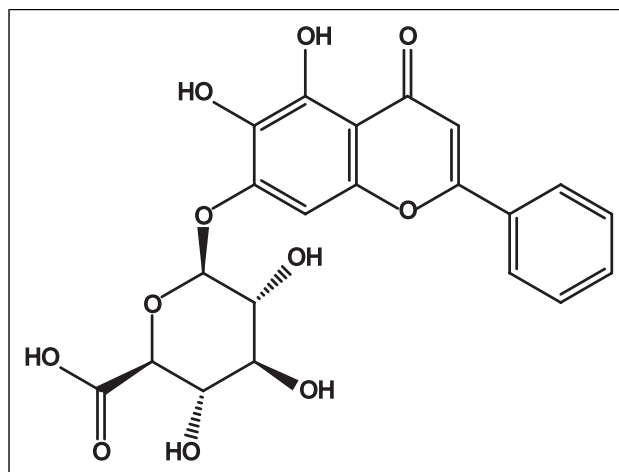


**Figure 1.** Chemical structure of baicalin.

transcription factors that play essential roles in inflammation, tissue survival, and carcinogenesis, including promoting anti-apoptosis, proliferation, and anti-stress effects.<sup>19</sup>

Effective activation of STAT3 is achieved under the influence of specific cytokines that signal Janus-kinase (JAK). The JAK family comprises non-transmembrane tyrosine kinases that phosphorylate the binding of cytokine receptors and a variety of SH2 region-specific signaling molecules. JAK2/STAT3 signaling plays a vital role in regulating different physiological functions at different stages of embryonic and adult development. Therefore, this pathway is one of the most important signaling pathways.<sup>20</sup> However, it is not clear whether it is involved in the protection by BA against ATO-induced acute liver injury. Thus, relevant experiments were conducted in this study to observe the protective effect of BA on ATO-induced acute liver injury and to explore its potential mechanism.

## Materials and methods

### Experimental chemicals

Arsenic trioxide was supplied by Shanghai Yuanye Biotechnology Co., Ltd. in China. Baicalin (purity >95%) was offered by Aladdin Biochemical Technology Co., Ltd. in China. Kits for detecting liver function markers and oxidative stress factors were purchased from the Nanjing Jiancheng Bioengineering Institute in China. The reagent for detecting As deposition was provided by Hebei Bio-high Technology Development CO., Ltd. in China. Unless otherwise specified, all other chemical reagents were analytical grade and furnished by Wuhan Servicebio Technology CO., Ltd. in China.

### Experimental objects

Fifty healthy male Kunming mice (weight,  $20 \pm 2$  g) were provided by Henan Skbex Biotechnology Co., Ltd. in

China. The mice were reared in an environment of 23–25°C and 40–60% relative humidity, and sufficient food and water were supplied. The experimental process was reviewed and ratified by the Animal Experimental Ethics Committee of Hebei University of Chinese Medicine (No. DWLL2020072).

### Experimental design

After a week of adaptation, all mice were divided into five groups stochastically (10 mice in each group, the number of mice was determined according to previous literatures<sup>21</sup>):

- ① CON group: all mice were treated with 0.9% normal saline at the same time as other groups
- ② ATO group: intragastric administration of 0.9% normal saline + intraperitoneal injection of 7.5 mg/kg of ATO
- ③ L-BA group: 50 mg/kg of BA by gavage + 7.5 mg/kg of ATO by intraperitoneal injection
- ④ H-BA group: 100 mg/kg of BA by gavage + 7.5 mg/kg of ATO by intraperitoneal injection
- ⑤ BA group: 100 mg/kg of BA by gavage + 0.9% normal saline by intraperitoneal injection

According to a preliminary experiment, the animal model of liver injury was successfully established by 7.5 mg/kg of ATO. Based on the literature, we selected 50 and 100 mg/kg of BA to perform the animal experiments.<sup>22,23</sup> Arsenic trioxide was injected intraperitoneally at 7 h after BA pretreatment. The entire course lasted for 7 days.

### Sample preparations

On the seventh day after administration, the water and food were removed, and the mice were fasted overnight. On the eighth day, the mice were killed with sodium pentobarbital (40 mg/kg) anesthesia. Blood was collected and put into heparinized vials. The serum was centrifuged and stored at –80°C for subsequent analysis. Some liver tissues were immersed in 4% paraformaldehyde solution, and the rest were frozen in liquid nitrogen at –196°C for analysis.

### Histological evolution

To assess the histopathological manifestations, the livers were harvested, fixed, and dehydrated with ethanol and embedded in paraffin. The specimens were cut into 4- $\mu$ m thick sections and stained with standard hematoxylin-eosin (H&E) and observed under a light microscope (Leica DM4000B).

### Assessment of hepatic injury

According to the instructions of the commercial diagnostic kits, we determined the activities of alanine aminotransferase (ALT), aspartate transaminase (AST), alkaline

phosphatase (ALP), and albumin (ALB) in serum. The degree of liver injury was evaluated by comparing the results of each treatment group.

### Detection of ROS by fluorescence microscopy

The level of ROS in the liver was evaluated with a dihydroethidium (DHE) fluorescence probe. The liver tissues were stained with DHE for 30 min at room temperature. After a series of reactions, the resulting ethidine oxide mixes into the DNA and produces red fluorescence. After washing with fresh solution, the fluorescence intensity was surveyed at an excitation wavelength of 535 nm and emission wavelength of 610 nm.

### Assay of oxidative and antioxidant indicators

A commercially available diagnostic kit for oxidative stress was applied according to the instructions. The activities of catalase (CAT), glutathione (GSH), malondialdehyde (MDA), and superoxide dismutase (SOD) in serum were assayed by a spectrophotometer.

### Enzyme-linked immunosorbent assay

According to the instructions of the Enzyme-linked immunosorbent assay (ELISA) kit, interleukin-1 $\beta$  (IL-1 $\beta$ ), interleukin-6 (IL-6), and tumor necrosis factor- $\alpha$  (TNF- $\alpha$ ) in liver tissue were detected as indicators of the inflammatory response during liver injury. We added 100  $\mu$ L of the properly diluted sample to the coated reaction well, sealed the plate, and incubated it at 37°C for 2 h. After washing five times, we added 100  $\mu$ L of the diluted biotinylated antibody working solution to each well, sealed the plate, and incubated it at 37°C for 1 h. Next, after washing five times, 100  $\mu$ L of the diluted enzyme conjugate working solution was added, followed by incubation at 37°C for 30 min in the dark.

After washing again, 100  $\mu$ L of TMB substrate solution was added to each well. The plate was reacted at 37°C for 30 min in darkness until a noticeable color gradient appeared in the standard well after dilution. Finally, 100  $\mu$ L of 2 M sulfuric acid was added to terminate the reaction. Within 10 min after the color change from blue to yellow was observed, the OD value of each well was measured at 450 nm on a microplate analyzer with respect to by setting the result of a blank control well, which was set as zero.

### TUNEL detection of apoptotic cells

Liver apoptosis was quantified by the terminal deoxynucleotidyl transferase dUTP nick end labeling (TUNEL) assay. Adequate dewaxing and hydration as well as appropriate cell permeability treatment were carried out. Sections were dried slightly, and freshly prepared 3,3'-diaminobenzidine

chromogenic reagent was added to the indicated tissue. Subsequently, hematoxylin was used to re-stain the slices. Finally, the slices were observed by optical microscope (magnification,  $\times 400$ ), dehydrated with alcohol hydrochloride, and blocked by neutral gel. Cells that stained brown in the nucleus indicate the occurrence of apoptosis.

### Western blot analysis

Liver tissue was homogenized and total protein was collected. The undenatured protein solution was measured with a bicinchoninic acid protein concentration determination kit according to the instructions. Equal amounts of denatured protein (30  $\mu\text{g}$ ) were separated on 10% SDS-PAGE gel and then transferred onto a 0.45- $\mu\text{m}$  PVDF membrane. The transferred protein was incubated with the primary antibodies (1:1000, dilution) and the secondary antibodies (1:3000, dilution) in turn. Antibodies: anti-Bcl-2 associated X protein (BAX) (Servicebio, Wuhan; GB11690), anti-B-cell lymphoma 2 (Bcl-2) (Cloud-clonal, Wuhan; PAA778Mu01), anti-caspase-3 (Proteintech Group, Wuhan; 66,470-2-Ig), anti-NF- $\kappa\text{B}$  (Servicebio, Wuhan; GB11142), anti-JAK2 (Servicebio, Wuhan; GB11325), anti-p-JAK2 (BIOSS, Beijing; BS-2485R), anti-STAT3 (Servicebio, Wuhan; GB11176), anti-p-STAT3 (Ruiying Biological, Jiangsu; RLP0250), and anti- $\beta$ -actin (Servicebio, Wuhan; GB12001).

The PVDF membrane protein was placed in an exposure box and mixed ECL solution was added for full reaction. After 2 min, the residual liquid was removed, and the film was pressed. The pressed film was developed and fixed with developing and fixing reagents. The exposure conditions were adjusted according to different luminous intensities. The film was then scanned and archived, Photoshop was used to decolor the film, and the Alpha software processing system was used to analyze the optical density of the target strip.

### Determination of mRNA by real time PCR

Total RNA was extracted from tissue samples using Trizol (ambion, 15,596,018). Reverse transcription with RT kit (CoWin Biosciences, CW2582 M) was performed. The target gene primers and internal reference gene primers were used for amplification at 60–95°C for the dissociation curve analysis. The target genes were detected using real-time PCR (BIO-RAD, CFX connect<sup>TM</sup>). Relative mRNA levels were calculated by the  $2^{-\Delta\Delta\text{Ct}}$  method. Primer sequences: caspase-3 forward AAGGAGCAGCTTTGTGTGTG, reverse TTCAACAGGCCATTGTCC; Bcl-2 forward GCTACCGTCGTGACTTCGCA, reverse CATCCAGCCTCCGT-TATCC; BAX forward GCCTTTTGTACAGGGTTTCAT, reverse TATTGCTGTCCAGTTCATCTCCA; actin forward TGCTTCGGGTTTGCATTTG, reverse AAGATCAC CCCC AAGATGACAC.

### Arsenic deposition in tissues

The samples were weighed and placed in the polytetrafluoroethylene digestion tube for pretreatment, added 0.5 mL hydrofluoric acid and 7 mL nitric acid mixed solution, and placed it in the digestion tank for 8 h (180°C). After complete dissolution and cooling, transfer to constant volume for instrument test (Agilent 7700 ICP-OES).

### Statistical analysis

The software SPSS 26.0 was used for statistical evaluation. The results were expressed as the mean  $\pm$  standard error of the mean (SEM), and differences between groups were measured by one-way analysis of variance or a student's t-test. We first conducted a normality test (Shapiro–Wilk test) and homogeneity test for the variance of each graph. When the data were not normally distributed, we used Mann–Whitney and Kruskal Wallis tests.  $p < 0.05$  indicates that a difference is statistically significant.

## Results

### Effects of BA on hepatic histological changes

In the histological analysis of ATO-induced liver injury (Figure 2), H&E staining of the central hepatic venous area showed that the histological structure of mice in the CON group was basically normal. The liver cells were arranged radially in a single line in the center of the central vein to form the hepatic plate. In the ATO group, the ATO-induced noticeable pathological changes in the liver tissue. The nuclei became larger. Edema and inflammatory cells increased. Massive cells were stained deeply. However, in the groups pretreated with BA, these phenomena were significantly improved. The improvement of the H-BA group was more obvious than that of the L-BA group. In the BA group, the sections were normal.

### Effects of BA on liver function

Several biochemical indexes in serum were selected to evaluate the liver function of mice in different treatment groups. Albumin and ALP were also measured to indicate liver function in addition to the two most commonly used indicators, ALT and AST. In the ATO group, the activities of ALT (Figure 3(a)), AST (Figure 3(b)), and ALP (Figure 3(c)) in the sera of mice were significantly increased compared to those in the CON group ( $p < 0.01$ ). There was no apparent change in the BA group treated with only 100 mg/kg BA. However, in the groups treated with ATO and BA, the activities of ALT, AST, and ALP were remarkably reduced compared with the ATO group ( $p < 0.01$ ).

Albumin reflects the protein anabolic function of hepatocytes. The ALB content was markedly lessened in the

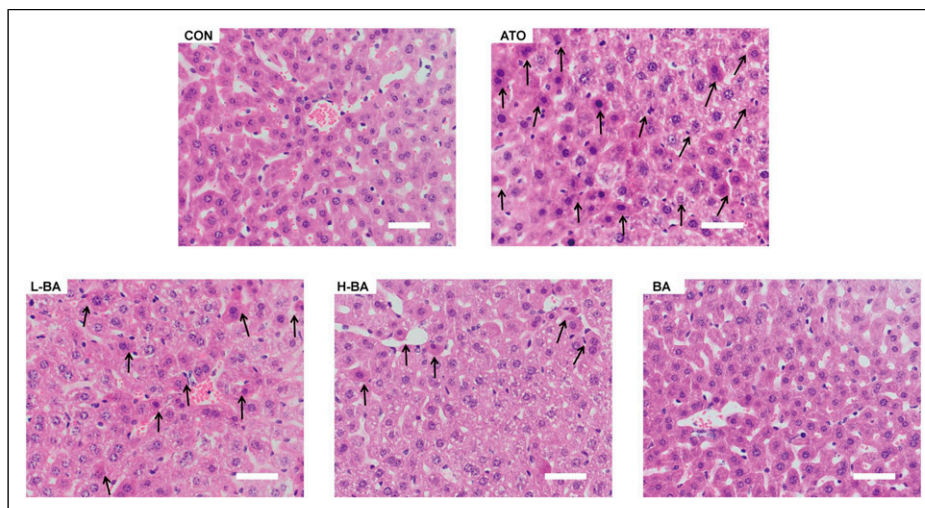


**Figure 2.** Histopathological examination of the liver by hematoxylin-eosin staining (magnification  $\times 400$ ). Typical sections of the hepatic central venous region in mice. Scale bar = 50  $\mu\text{m}$ . Abbreviations: CON: control group; ATO: arsenic trioxide-treated group; L-BA: low-dose baicalin group; H-BA: high-dose baicalin group; BA: baicalin alone group.

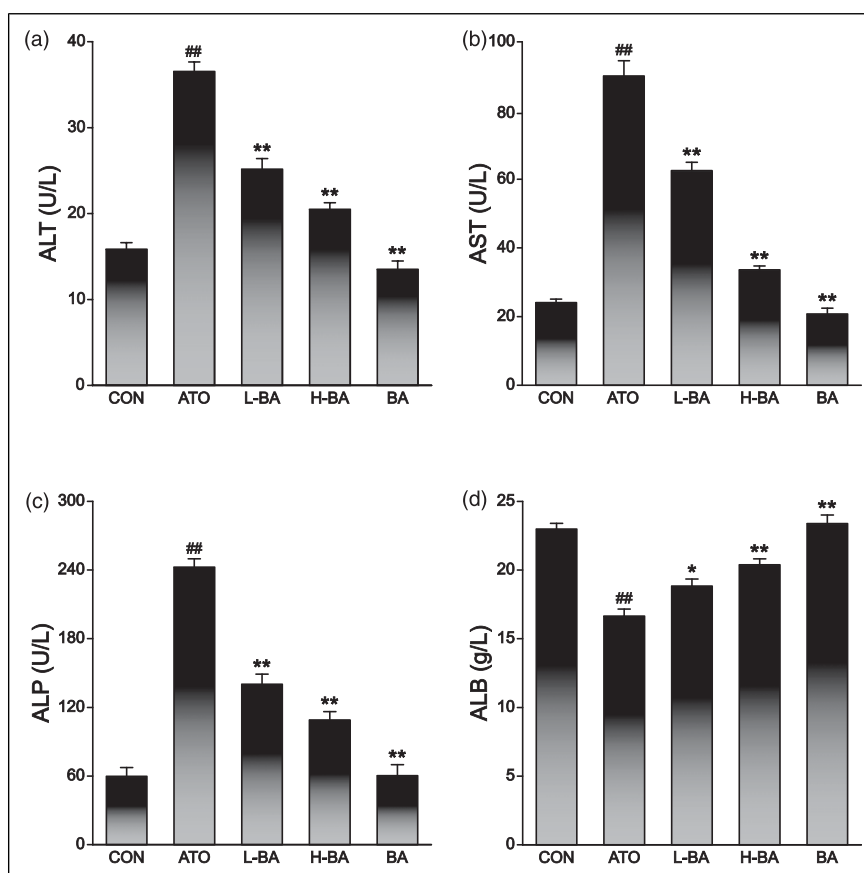


**Figure 3.** Effects of BA on ATO-induced changes in hepatic biomarkers. (a) ALT, (b) AST, (c) ALP, (d) ALB levels in serum of mice. The results are rendered by the mean  $\pm$  SEM ( $n = 5$ ).  $##p < 0.01$  compared with the CON group,  $*p < 0.05$  and  $**p < 0.01$  compared with the ATO group. Abbreviations: CON: control group; ATO: arsenic trioxide-treated group; L-BA: low-dose baicalin group; H-BA: high-dose baicalin group; BA: baicalin alone group. ALT: alanine aminotransferase; AST: aspartate transaminase; ALP: alkaline phosphatase; ALB: albumin; SEM: standard error of the mean.

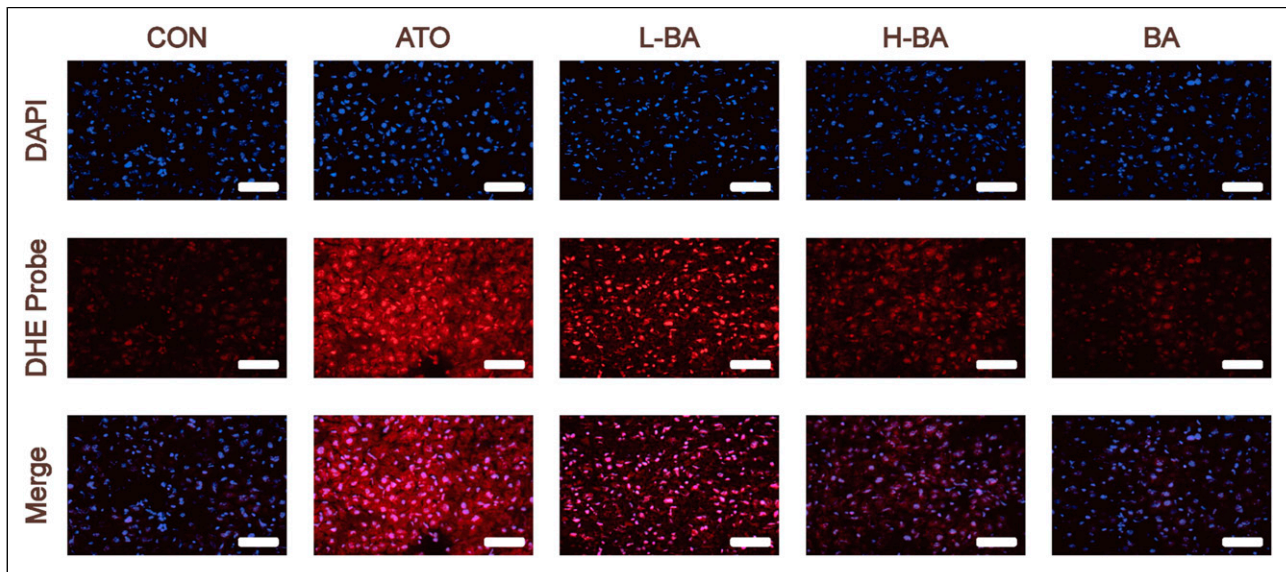


**Figure 4.** Production of ROS evaluated by detecting the fluorescence intensity of DHE-stained liver sections (magnification  $\times 400$ ). Scale bar = 50  $\mu\text{m}$ . Abbreviations: CON: control group; ATO: arsenic trioxide-treated group; L-BA: low-dose baicalin group; H-BA: high-dose baicalin group; BA: baicalin alone group; DHE: dihydroethidium.

ATO group ( $p < 0.01$ ) in comparison with the CON group (Figure 3(d)), while there was no significant change in the BA group. Compared with the ATO group, the ALB content was increased in the two groups treated with different doses of BA ( $p < 0.05$  or  $p < 0.01$ ).

#### Influences of BA on ROS production

Dihydroethylsulfur is used as a probe to detect ROS generated by living cells. The amount of ROS is indicated by the detected red fluorescence. As shown in Figure 4, the detection results of the ATO group showed a large amount of red fluorescence, meaning that a large amount of ROS was produced. However, only a spot of ROS was produced in the CON and BA groups. Compared with the ATO group, the red fluorescence intensity of the groups pretreated with BA was lower, indicating a decrease of ROS.

#### Effects of BA on antioxidant indexes

The contents of CAT, GSH, MDA, and SOD in serum were determined to evaluate the antioxidant effect of BA. As shown in Figure 5, the ATO group showed an obvious decrease in the levels of CAT (Figure 5(a)), SOD (Figure 5(b)), and GSH (Figure 5(d)) in the serum compared with those in the CON group. In contrast, the levels of the lipid peroxidation marker MDA increased significantly (Figure 5(c)) ( $p < 0.01$ ). In the other two groups treated with ATO and BA, the contents of CAT, GSH, and SOD were all increased compared with the ATO group ( $p < 0.05$  or  $p < 0.01$ ), while the content of MDA was decreased ( $p < 0.05$  or

$p < 0.01$ ). There was no obvious difference in the contents of these indexes between the CON group and the BA group.

#### Effects of BA on inflammatory cytokines levels

The levels of inflammatory cytokines are shown in Figure 6. Between the CON and BA groups, there was no visible difference in hepatic IL-1 $\beta$ , IL-6, TNF- $\alpha$ , and NF- $\kappa$ B levels. The expression levels of both in the ATO group were distinctly higher than those in the CON group ( $p < 0.01$ ). However, the overexpression of IL-1 $\beta$ , IL-6, TNF- $\alpha$ , and NF- $\kappa$ B was significantly reduced in liver tissues pretreated with 50 or 100 mg/kg of BA ( $p < 0.05$  or  $p < 0.01$ ).

#### Influences of BA on apoptosis

Apoptotic cells were detected using TUNEL staining, as shown in Figure 7. A small number of TUNEL-positive cells were observed in liver tissues of the CON and BA group, which showed normal apoptosis. However, a large area of brown was observed in the liver tissues of the ATO group, especially near the veins, which directly reflected an increase of apoptosis induced by ATO. Compared with the ATO group, the number of TUNEL-positive cells was markedly decreased in the BA-pretreated group.

Combined with mRNA determination (Figure 8) and protein expression levels (Figure 9), the detection results showed that compared with the CON group, there was no distinct difference in liver indexes of mice that only

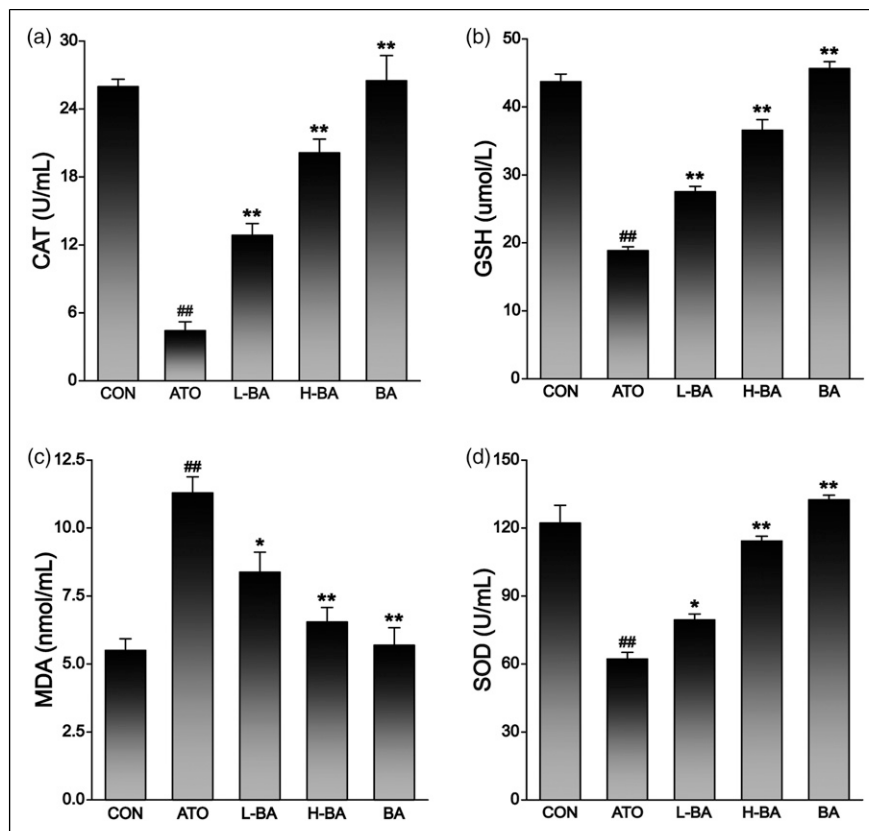


**Figure 5.** Effects of BA on ATO-induced changes in oxidative stress index. (a) CAT, (b) GSH, (c) MDA, (d) SOD levels in sera of mice. The results are rendered by the mean  $\pm$  SEM ( $n = 5$ ). ## $p < 0.01$  compared with the CON group, \* $p < 0.05$  and \*\* $p < 0.01$  compared with the ATO group. Abbreviations: CON: control group; ATO: arsenic trioxide-treated group; L-BA: low-dose baicalin group; H-BA: high-dose baicalin group; BA: baicalin alone group; CAT: catalase; GSH: glutathione; MDA: malondialdehyde; SOD: superoxide dismutase; SEM: standard error of the mean.

received 100 mg/kg of BA. The expression of Bcl-2 gene showed a remarkable decrease in the ATO group. However, the expressions of BAX and caspase-3 gene were observably increased ( $p < 0.01$ ). After pre-supplementation at 50 or 100 mg/kg, BA revitalized Bcl-2 and abated the BAX and caspase-3 of the ATO-induced mice ( $p < 0.05$  or  $p < 0.01$ ).

### Effects of BA on the expression of JAK2/STAT3 signal pathway

Some critical proteins in the JAK2/STAT3 signaling pathway were examined to investigate whether the mechanisms of action of BA are related to this pathway. The results (Figure 10) showed that compared with the CON group, the expression of p-JAK2 and p-STAT3 increased in the ATO group ( $p < 0.01$ ), while there was no significant change in the BA group. Compared with the ATO group, the expressions of both proteins were significantly enhanced in the two groups pretreated with BA ( $p < 0.01$ ).

### Effect of BA on ATO accumulation in liver

The total As deposition in the liver of mice in the ATO group was significantly higher than that of the CON group (Figure 11). However, BA pre-administration improved As metabolism, and significantly attenuated As retention in the liver ( $p < 0.05$  or  $p < 0.01$ ).

## Discussion

At present, the medical application of As has been widely recognized.<sup>24</sup> However, the toxicity of As and its compounds to the liver deserves our attention. As an important flavonoid in the rhizome of *Scutellaria baicalensis* Georgi, a number of experiments have shown that BA has significant anti-inflammatory and anti-oxidative stress effects in a variety of liver diseases. Thus, it is well-founded to deduce that BA has a phylactic effect against ATO-induced acute liver injury. Thereupon, the aim of the present study was to confirm the ameliorating effect of BA on ATO-induced liver injury in mice and the potential mechanism of the effect (Figure 12).

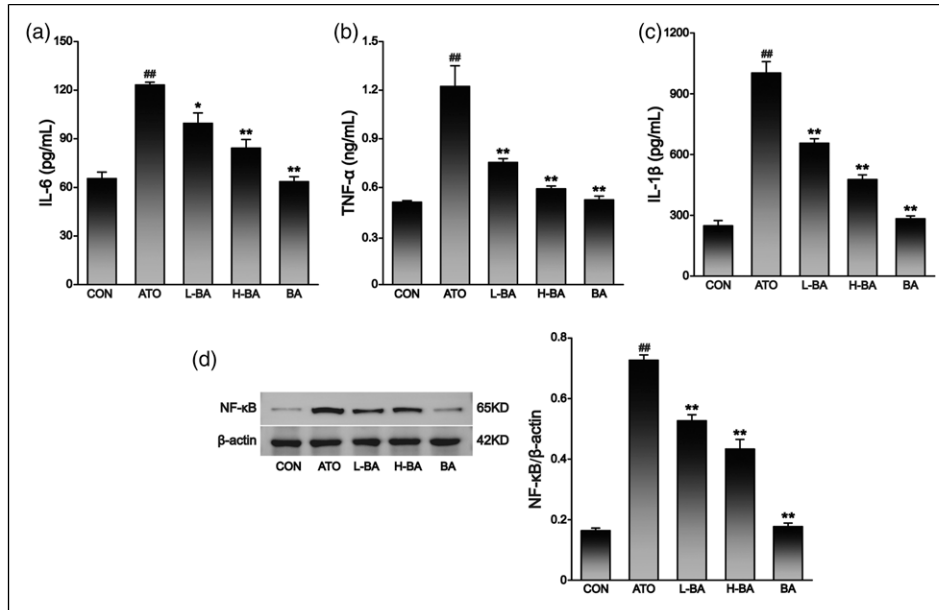


**Figure 6.** Effects of BA on ATO-induced changes in inflammatory factors analyzed by ELISA. Expression levels of (a) IL-6 and (b) TNF- $\alpha$ , and (c) IL-1 $\beta$  in liver tissue of mice. (d) Expression level of NF- $\kappa$ B in liver tissues assessed by Western-blot analysis and content of protein bands. The results are rendered by the mean  $\pm$  SEM ( $n = 3$ ).  $##p < 0.01$  compared with the CON group,  $*p < 0.05$  and  $**p < 0.01$  compared with the ATO group. Abbreviations: CON: control group; ATO: arsenic trioxide-treated group; L-BA: low-dose baicalin group; H-BA: high-dose baicalin group; BA: baicalin alone group; ELISA: Enzyme-linked immunosorbent assay; IL-1 $\beta$ : interleukin-1 $\beta$ ; IL-6: interleukin-6; TNF- $\alpha$ : tumor necrosis factor- $\alpha$ ; SEM: standard error of the mean.

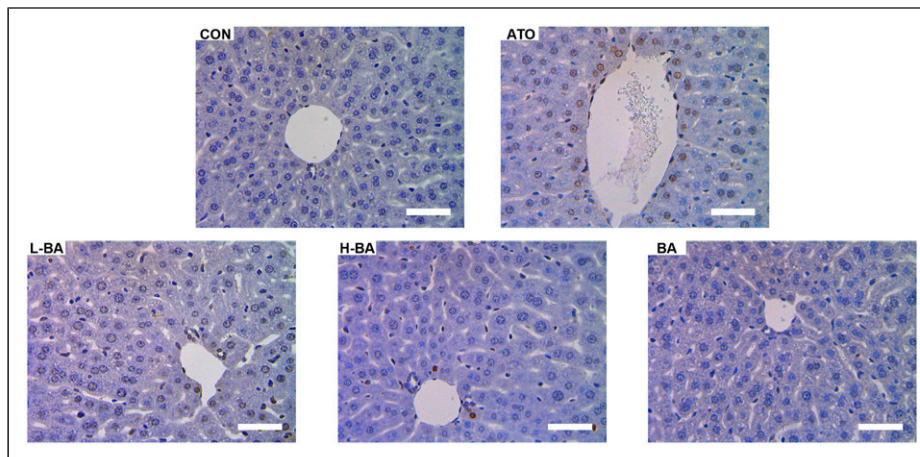


**Figure 7.** Apoptosis of mice liver cells analyzed by TUNEL staining. Brown color indicates hepatocyte apoptosis (magnification  $\times 400$ ). Scale bar = 50  $\mu$ m. Abbreviations: CON: control group; ATO: arsenic trioxide-treated group; L-BA: low-dose baicalin group; H-BA: high-dose baicalin group; BA: baicalin alone group.

Alanine aminotransferase and AST are generally considered representative indicators of liver injury because they typically enter the bloodstream after the structural integrity of liver cells is compromised.<sup>25</sup> In addition, ALP also enters the bloodstream through the lymphatic passages and sinuses. Albumin is synthesized by liver parenchymal cells, and its level reflects the protein synthesis function of liver cells.<sup>26</sup> The results showed that the serum indexes

were abnormal. Combined with the observation of pathological sections, ATO-induced serious liver injury.

Nithyanathan et al. showed that the toxicity of ATO to a normal liver causes not only massive histological changes but also severe oxidative stress.<sup>27</sup> Therefore, we examined ROS fluorescence and four serum indicators associated with oxidative stress, including three antioxidant enzymes and an oxidative intermediate. The results in this study



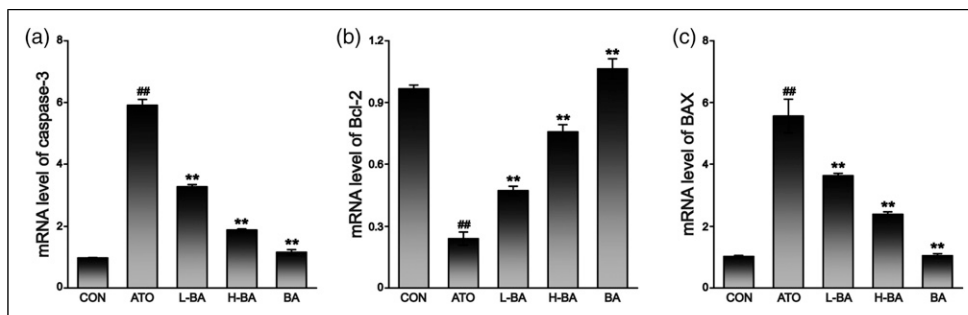


**Figure 8.** mRNA level of (a) caspase-3, (b) Bcl-2, and (c) BAX in liver tissues assessed by real time PCR. The results are rendered by the mean  $\pm$  SEM ( $n = 3$ ).  $###p < 0.01$  compared with the CON group,  $*p < 0.05$  and  $**p < 0.01$  compared with the ATO group. Abbreviations: CON: control group; ATO: arsenic trioxide-treated group; L-BA: low-dose baicalin group; H-BA: high-dose baicalin group; BA: baicalin alone group; SEM: standard error of the mean.

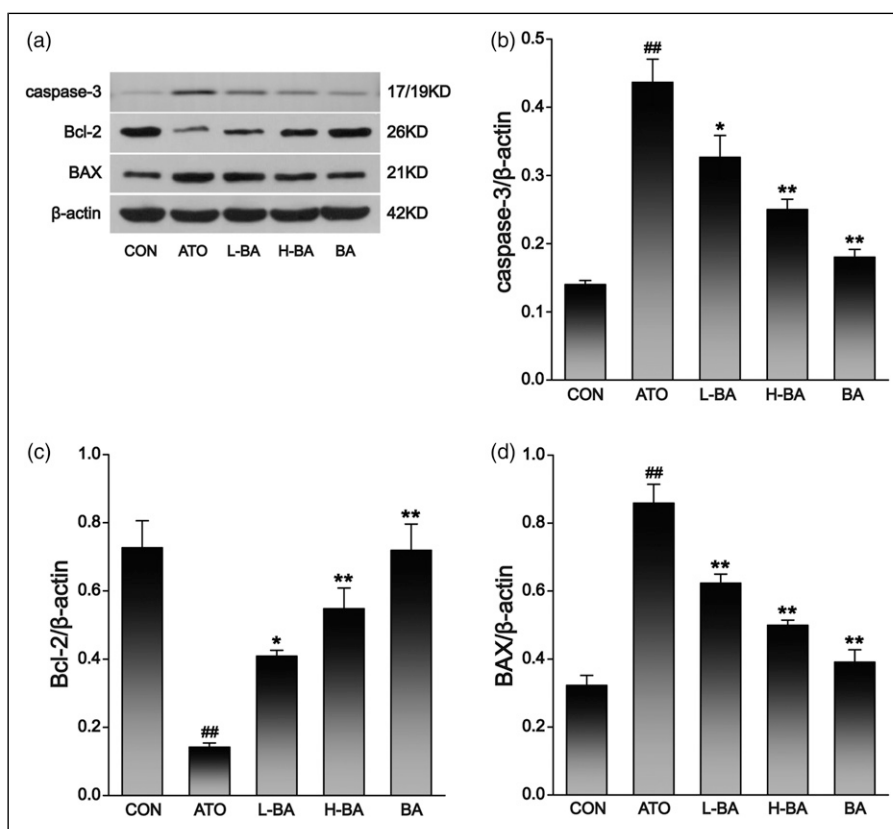


**Figure 9.** (a) Expression level of apoptotic factors in liver tissues assessed by Western-blot analysis and content of (b) caspase-3, (c) Bcl-2, and (d) BAX protein bands. The results are rendered by the mean  $\pm$  SEM ( $n = 3$ ).  $###p < 0.01$  compared with the CON group,  $*p < 0.05$  and  $**p < 0.01$  compared with the ATO group. Abbreviations: CON: control group; ATO: arsenic trioxide-treated group; L-BA: low-dose baicalin group; H-BA: high-dose baicalin group; BA: baicalin alone group; SEM: standard error of the mean.

were consistent with previous studies, indicating that ATO could cause severe oxidative stress in hepatocytes by producing excessive ROS production.

Oxidative stress can activate other reactions related to immunosuppression in vivo. ROS are the general toxic mediators by which inflammatory cells kill their targets,

and the formation of ROS in response to cytokine-induced stress signals in parenchymal cells also further mobilizes the cellular defense system.<sup>28</sup> When the liver is challenged by stimuli, inflammation usually occurs to protect it from injury. Hepatic inflammation acts as a critical driver of liver pathology when it persists or is out of

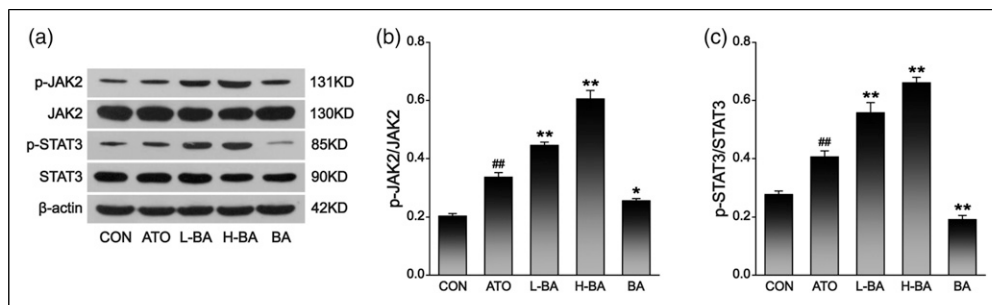


**Figure 10.** Effects of BA on JAK2/STAT3 signaling pathway in ATO-induced mice. (a) Western blot analysis was used to assess the hepatic protein expression levels of JAK2, p-JAK2, STAT3, and p-STAT3. (b) The relative expression level of p-JAK2. (c) The relative expression level of p-STAT3. The results are rendered by the mean  $\pm$  SEM ( $n = 3$ ). ### $p < 0.01$  compared with the CON group, \* $p < 0.05$  and \*\* $p < 0.01$  compared with the ATO group. Abbreviations: CON: control group; ATO: arsenic trioxide-treated group; L-BA: low-dose baicalin group; H-BA: high-dose baicalin group; BA: baicalin alone group; SEM: standard error of the mean.

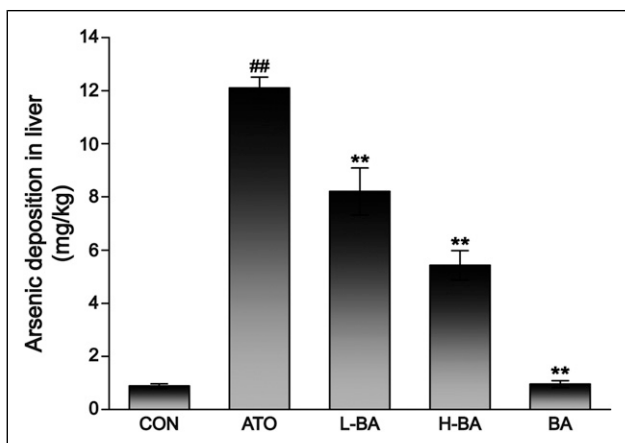


**Figure 11.** Effect of BA on ATO accumulation in liver. Arsenic deposition in the liver tissues of mice was determined using hydride generation-atomic fluorescence spectrometry. The analytical peaks obtained were quantified in terms of peak area by standard calibration. The results are rendered by the mean  $\pm$  SEM ( $n = 3$ ). ### $p < 0.01$  compared with the CON group, \* $p < 0.05$  and \*\* $p < 0.01$  compared with the ATO group. Abbreviations: CON: control group; ATO: arsenic trioxide-treated group; L-BA: low-dose baicalin group; H-BA: high-dose baicalin group; BA: baicalin alone group; SEM: standard error of the mean.

control.<sup>29</sup> Studies have shown that inflammatory response clusters include IL-1 $\beta$ , IL-6, TNF- $\alpha$ , and NF- $\kappa$ B, which are closely related to oxidative stress clusters.<sup>30</sup> As an initiator of excessive inflammation, TNF- $\alpha$  plays a major role in the inflammatory response.<sup>31</sup> Tumor necrosis factor- $\alpha$  and IL-1 $\beta$  activate signaling cascades that lead to the activation of NF- $\kappa$ B transcription factor, which regulate the transcription of downstream pro-inflammatory cytokine genes in the nucleus. In the initial stage of inflammation, IL-6 enters the liver through the bloodstream after it is synthesized in a localized lesion, which is

rapidly followed by the induction of large amounts of acute-phase proteins.<sup>32</sup> Therefore, we measured them, and the results showed that the expression of these inflammatory factors increased significantly under the action of ATO.

Oxidative stress is also an important factor in inducing programmed cell death. Mitochondria are the main source of ROS, and it also produces ATP.<sup>33</sup> Mitochondrial dysfunction can cause energy consumption and endogenous ROS production, while ROS overload makes mitochondrial damage more serious. Most apoptotic signals come from mitochondria, which are accused of being the central executioner of cell death.<sup>34</sup> Both the *BAX* and *Bcl-2* genes are the key genes in the regulation of apoptosis. In addition, caspase-3 is an “effector” protease in the cascade of apoptosis.<sup>35,36</sup> Therefore, the expression levels of the above three genes were determined in this experiment. The results showed that the expression of *Bcl-2* was significantly decreased, and the levels of *BAX* and caspase-3 were increased in the ATO group, which confirmed that ATO induced the apoptosis of liver cells. Apoptosis is the direct cause of tissue injury, including tissue dysfunction and structural disorder.

Pretreatment with BA remarkably improved the oxidative stress response induced by ATO, significantly reduced the accumulation of As in the liver, reduced the production of peroxidation products, and enhanced the antioxidant capacity, thereby reducing inflammation and improving cell apoptosis. Besides, the results showed that BA decreased the ATO deposition in the liver. After 7 days of pretreatment, the high dose BA reduced the percentage of As deposition by more than 55% compared with the ATO group. Reducing As deposits is a key to the treatment of As poisoning diseases.

The JAK2/STAT3 signaling pathway plays an important role in regulating apoptosis, proliferation, differentiation, and the inflammatory response.<sup>37-39</sup> The liver is a very

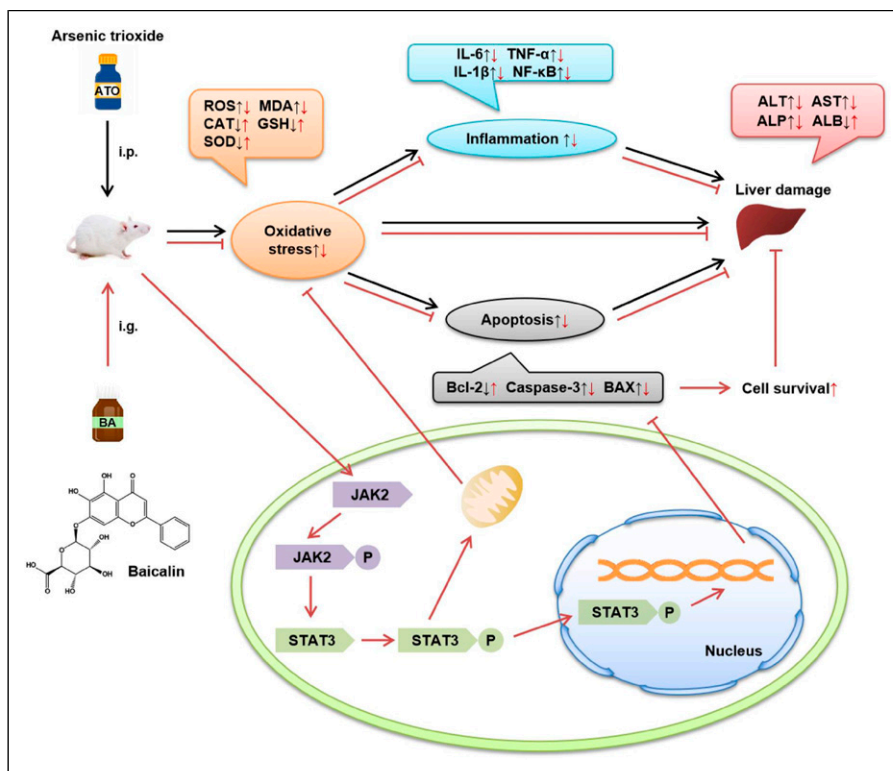


**Figure 12.** The mechanism of protection by BA against ATO-induced hepatotoxicity. ATO: arsenic trioxide-treated group; BA: baicalin alone group.

special organ that has evolved a powerful regenerative capacity to maintain homeostasis. Therefore, it is worth studying whether this pathway is involved in the protective effect of BA on the liver. The results showed that the expression of proteins related to the pathway was increased in the ATO group in comparison with the CON group. After pretreatment with BA, the expression of the associated proteins was significantly higher than that in the ATO group. This change indicates that the JAK2/STAT3 signaling pathway is involved in the protective effect of BA on ATO-induced acute liver injury.

Studies indicate that the expression of STAT3 gene could to a certain extent inhibit the NF-κB signaling pathway and reduce the inflammatory responses. In addition, inflammatory factors that activate the JAK/STAT pathway, such as the IL-6 and TNF-α, can inhibit the expression of the cytokine signaling pathway (SOCS) protein and pro-apoptotic factor BAX, as well as stimulate the expression of anti-apoptotic factor Bcl-2.<sup>40,41</sup> This also proves that BA can play a role in reducing inflammation and apoptosis by activating the JAK2/STAT3 signaling pathway. However, down-regulation of the pathway has also been shown to have a protective effect on the liver, such as in the stage of liver fibrosis or liver cancer.<sup>42-44</sup> These factors require contemplation, but they can explain

that the JAK2/STAT3 signal pathway must be involved in BA's effects against ATO-induced liver injury.

Combined with the powerful repair function of the liver, we hypothesized that the expression of the JAK2/STAT3 signaling pathway increases during acute injury. Pretreatment with BA can temporarily enhance this effect when induced by ATO.<sup>45</sup> As disease develops and reaches different stages, the direction of the regulation of each pathway might change.<sup>46,47</sup> When the liver is stimulated by acute toxins, it suddenly becomes disorganized. The liver tries to maintain homeostasis and reduce damage, and the inflammatory response is a self-protection mechanism for the liver. At this time, the JAK2/STAT3 signaling pathway is dominated by inflammatory factor activation. If the inflammation persists for too long, it can lead to fibrosis.<sup>48</sup>

To avoid an excessive inflammatory reaction and abnormal proliferation of hepatocytes, the protective effect of BA on the liver may be involve down-regulation of the expression of the JAK2/STAT3 signaling pathway.<sup>49-51</sup> This suggests that BA may achieve a protective effect on the liver through bidirectional regulation of the JAK2/STAT3 signaling pathway. Nevertheless, the mutual cooperation between multiple pathways in an organism is very complex, so it is necessary to study the actual situation in different animal models.

## Conclusion

In summary, this study has proven that BA achieves protective effects on ATO-induced acute liver injury by improving oxidative stress, reducing inflammation, and cell apoptosis. Furthermore, the results preliminarily proved that the JAK2/STAT3 signaling pathway is involved in the protective effect. Nevertheless, the specific regulatory mechanism requires further study.

## Declaration of conflicting interests

The author(s) declared no potential conflicts of interest with respect to the research, authorship, and/or publication of this article.

## Funding

The authors disclosed receipt of the following financial support for the research, authorship, and/or publication of this article: This work got support from the Research Foundation of the Administration of Traditional Chinese Medicine of Hebei Province, China [No.2019135].

## Ethics approval

Ethical approval for this study was obtained from the Animal Experimental Ethics Committee of Hebei University of Chinese Medicine (approval number: DWLL2020072).

## Animal welfare

The present study followed the Guidelines of Animal Experiments from the Committee of Medical Ethics for humane animal treatment and complied with relevant legislation.

## ORCID iDs

Li Chu  <https://orcid.org/0000-0002-6301-2709>

Shengjiang Guan  <https://orcid.org/0000-0003-3743-2870>

## References

- Alarifi S, Ali D, Alkahtani S, et al. (2013) Arsenic trioxide-mediated oxidative stress and genotoxicity in human hepatocellular carcinoma cells. *OncoTargets and Therapy* 6: 75–84. doi: [10.2147/OTT.S38227](https://doi.org/10.2147/OTT.S38227).
- Miller WH, Schipper HM, Lee JS, et al. (2002) Mechanisms of action of arsenic trioxide. *Cancer Research* 62(14): 3893–3903.
- Coombs CC, Tavakkoli M and Tallman MS (2015) Acute promyelocytic leukemia: where did we start, where are we now, and the future. *Blood Cancer Journal* 5: e304. DOI: [10.1038/bcj.2015.25](https://doi.org/10.1038/bcj.2015.25).
- Kaur T, Singh A and Goel R (2011) Mechanisms pertaining to arsenic toxicity. *Toxicology International* 18(2): 87. DOI: [10.4103/0971-6580.84258](https://doi.org/10.4103/0971-6580.84258).
- Real M, Barnhill MS, Higley C, et al. (2019) Drug-induced liver injury: highlights of the recent literature. *Drug Safety* 42(3): 365–387. DOI: [10.1007/s40264-018-0743-2](https://doi.org/10.1007/s40264-018-0743-2).
- Mazumder DN (2005) Effect of chronic intake of arsenic-contaminated water on liver. *Toxicology and Applied Pharmacology* 206(2): 169–175. DOI: [10.1016/j.taap.2004.08.025](https://doi.org/10.1016/j.taap.2004.08.025).
- Zhong G, Wan F, Yan H, et al. (2020) Methionine sulfoxide reductases are related to arsenic trioxide-induced oxidative stress in mouse liver. *Biological Trace Element Research* 195(2): 535–543. DOI: [10.1007/s12011-019-01881-6](https://doi.org/10.1007/s12011-019-01881-6).
- Burnett AK, Russell NH, Hills RK, et al. (2015) Arsenic trioxide and all-trans retinoic acid treatment for acute promyelocytic leukaemia in all risk groups (AML17): results of a randomised, controlled, phase 3 trial. *The Lancet Oncology* 16(13): 1295–1305. DOI: [10.1016/S1470-2045\(15\)00193-X](https://doi.org/10.1016/S1470-2045(15)00193-X).
- Lo-Coco F, Avvisati G, Vignetti M, et al. (2013) Retinoic acid and arsenic trioxide for acute promyelocytic leukemia. *The New England journal of medicine* 369(2): 111–121. DOI: [10.1056/NEJMoa1300874](https://doi.org/10.1056/NEJMoa1300874).
- Zhao Q, Chen XY and Martin C (2016) Scutellaria baicalensis, the golden herb from the garden of Chinese medicinal plants. *Science Bulletin* 61(18): 1391–1398. DOI: [10.1007/s11434-016-1136-5](https://doi.org/10.1007/s11434-016-1136-5).
- de Oliveira MR, Nabavi SF, Habtemariam S, et al. (2015) The effects of baicalein and baicalin on mitochondrial function and dynamics: a review. *Pharmacological Research* 100: 296–308. DOI: [10.1016/j.phrs.2015.08.021](https://doi.org/10.1016/j.phrs.2015.08.021).
- Xiping Z, Jie Z, Qin X, et al. (2009) Influence of baicalin and octreotide on NF-κB and P-selectin expression in liver and kidney of rats with severe acute pancreatitis. *Inflammation* 32(1): 1–11. DOI: [10.1007/s10753-008-9096-9](https://doi.org/10.1007/s10753-008-9096-9).
- Liu J, Yuan Y, Gong X, et al. (2020) Baicalin and its nanoliposomes ameliorates nonalcoholic fatty liver disease via suppression of TLR4 signaling cascade in mice. *International Immunopharmacology* 80: 106208. DOI: [10.1016/j.intimp.2020.106208](https://doi.org/10.1016/j.intimp.2020.106208).
- Zhang Y, Huang Y, Deng X, et al. (2012) Iron overload-induced rat liver injury: involvement of protein tyrosine nitration and the effect of baicalin. *European Journal of Pharmacology* 680(1–3): 95–101. DOI: [10.1016/j.ejphar.2012.01.010](https://doi.org/10.1016/j.ejphar.2012.01.010).
- Wang H, Zhang Y, Bai R, et al. (2016) Baicalin attenuates alcoholic liver injury through modulation of hepatic oxidative stress, inflammation and sonic hedgehog pathway in rats. *Cellular Physiology and Biochemistry* 39(3): 1129–1140. DOI: [10.1159/000447820](https://doi.org/10.1159/000447820).
- Kim SJ, Moon YJ and Lee SM (2010) Protective effects of baicalin against ischemia/reperfusion injury in rat liver. *Journal of Natural Products* 73(12): 2003–2008. DOI: [10.1021/np100389z](https://doi.org/10.1021/np100389z).
- Shen K, Feng X, Pan H, et al. (2017) Baicalin ameliorates experimental liver cholestasis in mice by modulation of oxidative stress, inflammation, and NRF2 transcription factor. *Oxidative Medicine and Cellular Longevity* 2017: 1–11. DOI: [10.1155/2017/6169128](https://doi.org/10.1155/2017/6169128).
- Mühl H (2016) STAT3, a Key parameter of cytokine-driven tissue protection during sterile inflammation-the case of

- experimental acetaminophen (paracetamol)-induced liver damage. *Frontiers in Immunology* 7: 163. DOI: [10.3389/fimmu.2016.00163](https://doi.org/10.3389/fimmu.2016.00163).
19. O'Shea JJ, Schwartz DM, Villarino AV, et al. (2015) The JAK-STAT pathway: impact on human disease and therapeutic intervention. *Annual Review of Medicine* 66: 311–328. DOI: [10.1146/annurev-med-051113-024537](https://doi.org/10.1146/annurev-med-051113-024537).
  20. Roskoski RJ (2016) Janus kinase (JAK) inhibitors in the treatment of inflammatory and neoplastic diseases. *Pharmacological Research* 111: 784–803. DOI: [10.1016/j.phrs.2016.07.038](https://doi.org/10.1016/j.phrs.2016.07.038).
  21. Sun X, Wang X, He Q, et al. (2021) Investigation of the ameliorative effects of baicalin against arsenic trioxide-induced cardiac toxicity in mice. *International Immunopharmacology* 99: 108024. DOI: [10.1016/j.intimp.2021.108024](https://doi.org/10.1016/j.intimp.2021.108024).
  22. Park S, Lee C, Kim YS, et al. (2008) Protective effect of baicalin against carbon tetrachloride-induced acute hepatic injury in mice. *Journal of Pharmacological Sciences* 106(1): 136–143. DOI: [10.1254/jphs.FP0071392](https://doi.org/10.1254/jphs.FP0071392).
  23. Hu Q, Zhang W, Wu Z, et al. (2021) Baicalin and the liver-gut system: pharmacological bases explaining its therapeutic effects. *Pharmacological Research* 165: 105444. DOI: [10.1016/j.phrs.2021.105444](https://doi.org/10.1016/j.phrs.2021.105444).
  24. Lazo G, Kantarjian H, Estey E, et al. (2003) Use of arsenic trioxide (As<sub>2</sub>O<sub>3</sub>) in the treatment of patients with acute promyelocytic leukemia: the M. D. Anderson experience. *Cancer* 97(9): 2218–2224. DOI: [10.1002/cncr.11314](https://doi.org/10.1002/cncr.11314).
  25. Vermeulen NP, Bessems JG and Van de Straat R (1992) Molecular aspects of paracetamol-induced hepatotoxicity and its mechanism-based prevention. *Drug Metabolism Reviews* 24(3): 367–407. DOI: [10.3109/03602539208996298](https://doi.org/10.3109/03602539208996298).
  26. Yu MC, Chan KM, Lee CF, et al. (2011) Alkaline phosphatase: does it have a role in predicting hepatocellular carcinoma recurrence? *Journal of Gastrointestinal Surgery* 15(8): 1440–1449. DOI: [10.1007/s11605-011-1537-3](https://doi.org/10.1007/s11605-011-1537-3).
  27. Nithyananthan S and Thirunavukkarasu C (2019) Chemotherapeutic doses of arsenic trioxide delays hepatic regeneration by oxidative stress and hepatocyte apoptosis in partial hepatectomy rat. *Toxicology and Applied Pharmacology* 382: 114760. DOI: [10.1016/j.taap.2019.114760](https://doi.org/10.1016/j.taap.2019.114760).
  28. Han B, Lv Z, Han X, et al. (2021) Harmful effects of inorganic mercury exposure on kidney cells: mitochondrial dynamics disorder and excessive oxidative stress. *Biological Trace Element Research*. doi: [10.1007/s12011-021-02766-3](https://doi.org/10.1007/s12011-021-02766-3).
  29. Sumedha NC and Miltonprabu S (2015) Diallyl trisulfide ameliorates arsenic-induced hepatotoxicity by abrogation of oxidative stress, inflammation, and apoptosis in rats. *Human & Experimental Toxicology* 34(5): 506–525. DOI: [10.1177/0960327114543933](https://doi.org/10.1177/0960327114543933).
  30. Zhang Z, Guo C, Jiang H, et al. (2020) Inflammation response after the cessation of chronic arsenic exposure and post-treatment of natural astaxanthin in liver: potential role of cytokine-mediated cell-cell interactions. *Food & Function* 11(10): 9252–9262. DOI: [10.1039/d0fo01223h](https://doi.org/10.1039/d0fo01223h).
  31. Tanaka T, Narazaki M and Kishimoto T (2014) IL-6 in inflammation, immunity, and disease. *Cold Spring Harbor Perspectives in Biology* 6(10): a016295. DOI: [10.1101/cshperspect.a016295](https://doi.org/10.1101/cshperspect.a016295).
  32. Luster MI (1998) Inflammation, tumor necrosis factor, and toxicology. *Environmental Health Perspectives* 106(9): A418–A419. DOI: [10.1289/ehp.98106a418](https://doi.org/10.1289/ehp.98106a418).
  33. Yang D, Yang Q, Fu N, et al. (2021) Hexavalent chromium induced heart dysfunction via Sesn2-mediated impairment of mitochondrial function and energy supply. *Chemosphere* 264(Pt 2): 128547. DOI: [10.1016/j.chemosphere.2020.128547](https://doi.org/10.1016/j.chemosphere.2020.128547).
  34. Han B, Li S, Lv Y, et al. (2019) Dietary melatonin attenuates chromium-induced lung injury via activating the Sirt1/Pgc-1α/Nrf2 pathway. *Food & Function* 10(9): 5555–5565. DOI: [10.1039/c9fo01152h](https://doi.org/10.1039/c9fo01152h).
  35. Engel RH and Evens AM (2006) Oxidative stress and apoptosis: a new treatment paradigm in cancer. *Frontiers in Bioscience* 11: 300–312. DOI: [10.2741/1798](https://doi.org/10.2741/1798).
  36. Adedara IA, Adebowale AA, Atanda OE, et al. (2019) Selenium abates reproductive dysfunction via attenuation of biometal accumulation, oxido-inflammatory stress and caspase-3 activation in male rats exposed to arsenic. *Environmental Pollution* 254(Pt B): 113079. DOI: [10.1016/j.envpol.2019.113079](https://doi.org/10.1016/j.envpol.2019.113079).
  37. Chatterjee-Kishore M, van den Akker F and Stark GR (2000) Association of STATs with relatives and friends. *Trends in Cell Biology* 10(3): 106–111. DOI: [10.1016/s0962-8924\(99\)01709-2](https://doi.org/10.1016/s0962-8924(99)01709-2).
  38. Kao J, Feng C, Yu C, et al. (2015) IL-6, through p-STAT3 rather than p-STAT1, activates hepatocarcinogenesis and affects survival of hepatocellular carcinoma patients: a cohort study. *BMC Gastroenterology* 15(1): 50. DOI: [10.1186/s12876-015-0283-5](https://doi.org/10.1186/s12876-015-0283-5).
  39. Chen HL, Tsai TC, Tsai YC, et al. (2016) Kefir peptides prevent high-fructose corn syrup-induced non-alcoholic fatty liver disease in a murine model by modulation of inflammation and the JAK2 signaling pathway. *Nutrition & Diabetes* 6(12): e237. DOI: [10.1038/ntud.2016.49](https://doi.org/10.1038/ntud.2016.49).
  40. Kong W, Shen F, Xie R, et al. (2021) Bufotionine induces autophagy in H22 hepatoma-bearing mice by inhibiting JAK2/STAT3 pathway, a possible anti-cancer mechanism of cinobufacini. *Journal of Ethnopharmacology* 270: 113848. DOI: [10.1016/j.jep.2021.113848](https://doi.org/10.1016/j.jep.2021.113848).
  41. Liu C, Zhao Q, Zhong L, et al. (2021) Tibetan medicine Ershiwuwei Lvxue Pill attenuates collagen-induced arthritis via inhibition of JAK2/STAT3 signaling pathway. *Journal of Ethnopharmacology* 270: 113820. DOI: [10.1016/j.jep.2021.113820](https://doi.org/10.1016/j.jep.2021.113820).
  42. Yang YZ, Zhao XJ, Xu HJ, et al. (2019) Magnesium isoglycyrrhizinate ameliorates high fructose-induced liver fibrosis in rat by increasing miR-375-3p to suppress JAK2/STAT3 pathway and TGF-β1/Smad signaling. *Acta*

- Pharmacologica Sinica* 40(7): 879–894. DOI: [10.1038/s41401-018-0194-4](https://doi.org/10.1038/s41401-018-0194-4).
43. Guha P, Gardell J, Darpolor J, et al. (2019) STAT3 inhibition induces Bax-dependent apoptosis in liver tumor myeloid-derived suppressor cells. *Oncogene* 38(4): 533–548. DOI: [10.1038/s41388-018-0449-z](https://doi.org/10.1038/s41388-018-0449-z).
  44. Li M, Zhang X, Wang B, et al. (2018) Effect of JAK2/STAT3 signaling pathway on liver injury associated with severe acute pancreatitis in rats. *Experimental and Therapeutic Medicine* 16(3): 2013–2021. DOI: [10.3892/etm.2018.6433](https://doi.org/10.3892/etm.2018.6433).
  45. Zai W, Chen W, Luan J, et al. (2018) Dihydroquercetin ameliorated acetaminophen-induced hepatic cytotoxicity via activating JAK2/STAT3 pathway and autophagy. *Applied Microbiology and Biotechnology* 102(3): 1443–1453. DOI: [10.1007/s00253-017-8686-6](https://doi.org/10.1007/s00253-017-8686-6).
  46. de Jonge WJ, van der Zanden EP, The FO, et al. (2005) Stimulation of the vagus nerve attenuates macrophage activation by activating the JAK2-STAT3 signaling pathway. *Nature Immunology* 6(8): 844–851. DOI: [10.1038/ni1229](https://doi.org/10.1038/ni1229).
  47. Wörmann SM, Song L, Ai J, et al. (2016) Loss of P53 function activates JAK2-STAT3 signaling to promote pancreatic tumor growth, stroma modification, and gemcitabine resistance in mice and is associated with patient survival. *Gastroenterology* 151(1): 180–193. DOI: [10.1053/j.gastro.2016.03.010](https://doi.org/10.1053/j.gastro.2016.03.010).
  48. Zhang J, Zhang H, Deng X, et al. (2018) Baicalin attenuates non-alcoholic steatohepatitis by suppressing key regulators of lipid metabolism, inflammation and fibrosis in mice. *Life Sciences* 192: 46–54. DOI: [10.1016/j.lfs.2017.11.027](https://doi.org/10.1016/j.lfs.2017.11.027).
  49. Ying XD, Wei G and An H (2021) Sodium butyrate relieves lung ischemia-reperfusion injury by inhibiting NF- $\kappa$ B and JAK2/STAT3 signaling pathways. *European Review for Medical and Pharmacological Sciences* 25(1): 413–422. DOI: [10.26355/eurrev\\_202101\\_24409](https://doi.org/10.26355/eurrev_202101_24409).
  50. Dong W, Xian Y, Yuan W, et al. (2016) Catalpol stimulates VEGF production via the JAK2/STAT3 pathway to improve angiogenesis in rats' stroke model. *Journal of Ethnopharmacology* 191: 169–179. DOI: [10.1016/j.jep.2016.06.030](https://doi.org/10.1016/j.jep.2016.06.030).
  51. Yang X, Gao X, Du B, et al. (2018) Ilex asprella aqueous extracts exert in vivo anti-inflammatory effects by regulating the NF- $\kappa$ B, JAK2/STAT3, and MAPK signaling pathways. *Journal of Ethnopharmacology* 225: 234–243. DOI: [10.1016/j.jep.2018.06.037](https://doi.org/10.1016/j.jep.2018.06.037).